Lecture notes:
Electron Monte Carlo simulation

Alex F Bielajew and D W O Rogers
Institute for National Measurement Standards
National Research Council of Canada
Ottawa, Canada
K1A 0R6

Tel: 613-993-2715
FAX: 613-952-9865
e-mail: alex@irs.phy.nrc.ca

National Research Council of Canada Report PIRS-0394

"Anyone who considers arithmetical methods of producing random digits is, of course, in a state of sin."
John von Neumann (1951)

1 Introduction

In this lecture we discuss the electron and positron interactions modeled by the standard EGS4 code with a view to discussing and appreciating the approximations made in their implementation. We briefly describe some non-standard EGS4 physics modeling that may be employed for specialised applications and give a brief outline of the electron transport logic used in EGS4.

The transport of electrons (and positrons) is considerably more complicated than for photons. Like photons, electrons are subject to violent interactions. The following "catastrophic" interactions are modeled by the standard EGS4 code:

- large energy-loss Møller scattering ($e^-e^- \longrightarrow e^-e^-$),
- large energy-loss Bhabha scattering ($e^+e^- \longrightarrow e^+e^-$),
- hard bremsstrahlung emission ($e^\pm\mathrm{N} \longrightarrow e^\pm\gamma\mathrm{N}$), and
- positron annihilation "in-flight" and at rest ($e^+e^- \longrightarrow \gamma\gamma$).

It is possible to sample these interactions discretely in a reasonable amount of computing time for many practical problems. In addition, standard EGS4 models electrons (positrons) interacting non-catastrophically via:

- low-energy Møller (Bhabha) scattering (as part of restricted collision stopping power),
- atomic excitation ($e^\pm\mathrm{N} \longrightarrow e^\pm\mathrm{N}^*$) (as the other part of restricted collision stopping power),
- soft bremsstrahlung (restricted radiative stopping power), and
- elastic electron (positron) multiple scattering from atoms, ($e^\pm\mathrm{N} \longrightarrow e^\pm\mathrm{N}$).

Strictly speaking, an elastic large angle scattering from a nucleus should really be considered to be a "catastrophic" interaction but this is not the convention of EGS4. (Perhaps one day it should be.) For problems of the sort we consider, it is impractical to model all these interactions discretely. Instead, well-established statistical theories are used to describe these "weak" interactions by accounting for them in a cumulative sense including the effect of many such interactions at the same time. These are the so-called "statistically grouped" interactions.

2 Catastrophic interactions

EGS4 has almost complete flexibility in defining the threshold between "catastrophic" and "statistically grouped" interactions. The location of this threshold should be chosen by the demands of the physics of the problem and by the accuracy required in the final result. Later in the lecture we give several examples of how setting transport parameters affects calculated results.

2.1 Hard bremsstrahlung production

As depicted in fig. 1, bremsstrahlung production is the creation of photons above the threshold `AP` by electrons (or positrons) in the field of an atom. (Variables expressed in teletype font, *e.g.* `AP`, refer directly to an EGS4 variable or a subroutine name.) There are actually two

possibilities. The predominant mode is the interaction with the atomic nucleus. This effect dominates by a factor of about Z^2 over the three-body case where an atomic electron recoils ($e^{\pm}\mathrm{N} \longrightarrow e^{\pm}e^{-}\gamma\mathrm{N}^{*}$). Bremsstrahlung is the quantum analogue of synchrotron radiation, the radiation from accelerated charges predicted by Maxwell's equations. The de-acceleration and acceleration of an electron scattering from nuclei can be quite violent, resulting in very high energy quanta, up to and including the total kinetic energy of the incoming charged particle.

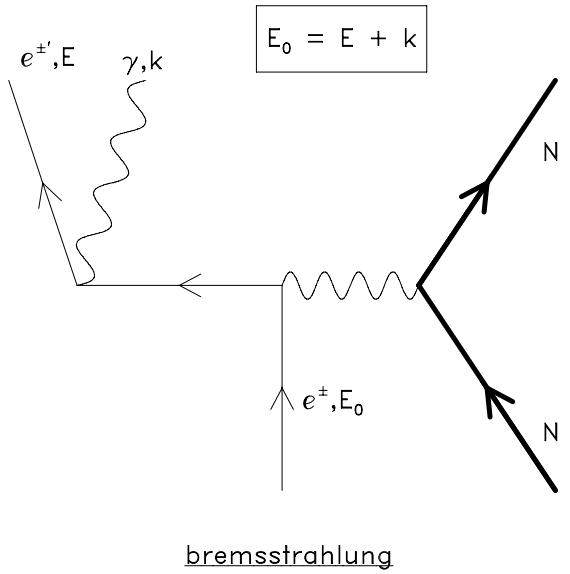

Figure 1: Hard bremsstrahlung production in the field of an atom. There are two possibilities. The predominant mode (shown here) is a two-body interaction where the nucleus recoils. This effect dominates by a factor of about Z^2 over the three-body case where an atomic electron recoils.

EGS4 takes the two-body effect into account through the total cross section and angular distribution kinematics. The three-body case is treated only by inclusion in the total cross section of the two body-process. The two-body process is modeled by the Koch and Motz [1] formulae (essentially the unscreened Born approximation). Below 50 MeV, empirical corrections to the total cross section are added to get agreement with experiment while at higher energies, extreme relativistic Coulomb corrected cross sections are employed. Thomas-Fermi screening factors are employed to model the screening of the nucleus by the orbital electrons. The Coulomb correction term is taken from Davies *et al.* [2]. The bremsstrahlung cross section scales with $Z(Z + \xi(Z))$, where $\xi(Z)$ is the factor accounting for three-body case where the interaction is with an atomic electron. These factors comes are taken from the work of Tsai [3]. The total cross section, as modeled by EGS4, depends approximately like $1/E_\gamma$.

Several important approximations are made in the modeling of bremsstrahlung in the EGS4 code:

- The infrared divergence ($1/E_\gamma$-dependence for small E_γ) is permitted to occur (although it is cut-off by the lower threshold for production by `AP`). This is not really the case due to polarisation of the medium and accurate treatment of screening at low energies. Problems which concern themselves with the low-energy photon spectrum will be affected although the effects will be masked by photons produced by copious low energy electrons in most problems. Thin targets are especially susceptible.

- EGS4 treats electrons and positrons as the same with respect to bremsstrahlung. Actually, at low energies, positron bremsstrahlung is suppressed relative to electron bremsstrahlung. Any study that depends upon accurate modeling of bremsstrahlung below 2 MeV electron energy will be affected.
- The three-body mode may be important in low-Z materials.
- "Suppression effects", important above 100 GeV, are ignored.
- The electron is not deflected by the bremsstrahlung interaction.
- Rather than sampling the bremsstrahlung photon's direction from a distribution, EGS4 sets it off in a direction uniquely defined by the energy, E_0, of the initiating electron, $\Theta_{\rm scat} = m_e/E_0$.
- EGS4's employment of the unscreened Born approximation forces the high-energy "bremsstrahlung tip" to zero when actually it has a finite value. The electron can actually convert all its kinetic energy into a radiative photon.

One should be aware that these shortcomings are inherent before undertaking any detailed bremsstrahlung study. Recently, Rogers *et al.* [4] have implemented new bremsstrahlung total cross sections by forcing the radiative stopping powers (essentially the energy-weighted integral over the cross section) to conform to ICRU 37 [5]. In fact, the capability of updating the radiative stopping powers to the state-of-the-art (as defined by the bremsstrahlung gurus, Seltzer and Berger [6]) is given. Further improvements in sampling the bremsstrahlung photon angular distribution from Koch and Motz [1] has been done by Bielajew *et al.* [7].

2.2 Møller (Bhabha) scattering

Møller and Bhabha scattering are hard collisions of incident electrons or positrons with atomic electrons. EGS4 assumes these atomic electrons to be free ignoring their atomic binding energy. At first glance the Møller and Bhabha interactions appear to be quite similar. Referring to fig. 2, we see very little difference between them. In reality, however, they are, owing to the

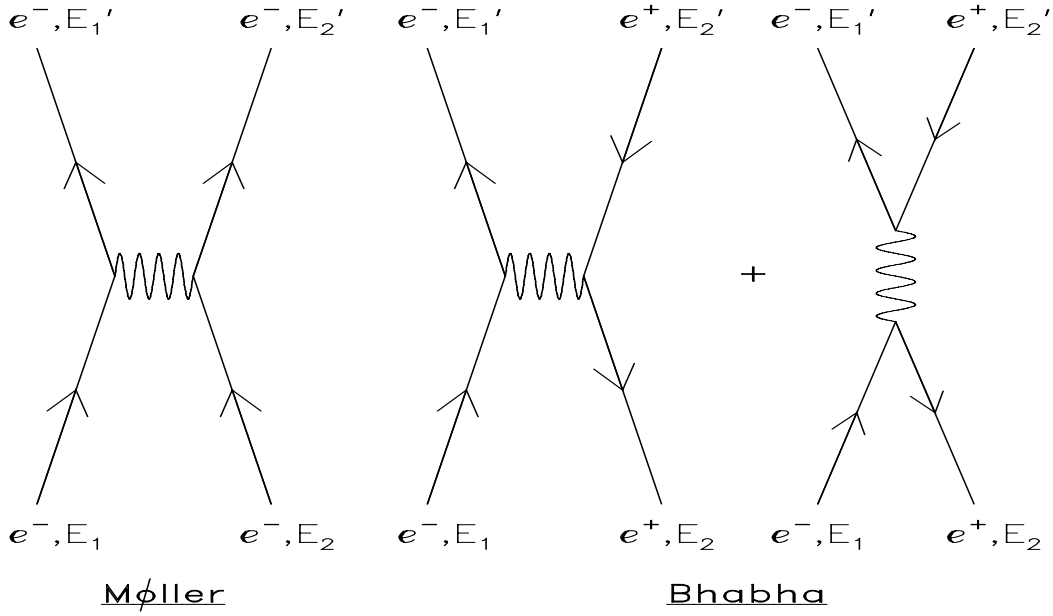

Figure 2: Møller and Bhabha interactions.

identity of the participant particles. The electrons in the e^-e^- pair can annihilate and be

recreated, contributing an extra interaction channel to the cross section. The thresholds for these interactions are different as well. In the e^-e^- case, the cross section goes to zero when the incident electron kinetic energy is `2*(AE-RM)`. This is because an electron's kinetic energy must be more twice the threshold (`AE` -`RM`) to produce another electron above this threshold and still remain above it. In the e^+e^- case the cross section goes all the way down to `AE`, because the particles are distinguishable. The positron can give up all its energy to the atomic electron.

Atomic corrections are ignored in these interactions. Therefore, one should insure that `AE` is larger (preferably much larger) than the highest K-shell energy of any medium in the problem. Møller and Bhabha cross sections scale with Z for different media. The cross section scales also scales approximately as $1/v^2$, where v is the velocity of the scattered electron. Many more low energy secondary particles are produced from the Møller interaction than from the bremsstrahlung interaction.

2.3 Positron annihilation

Two photon annihilation is depicted in fig. 3.

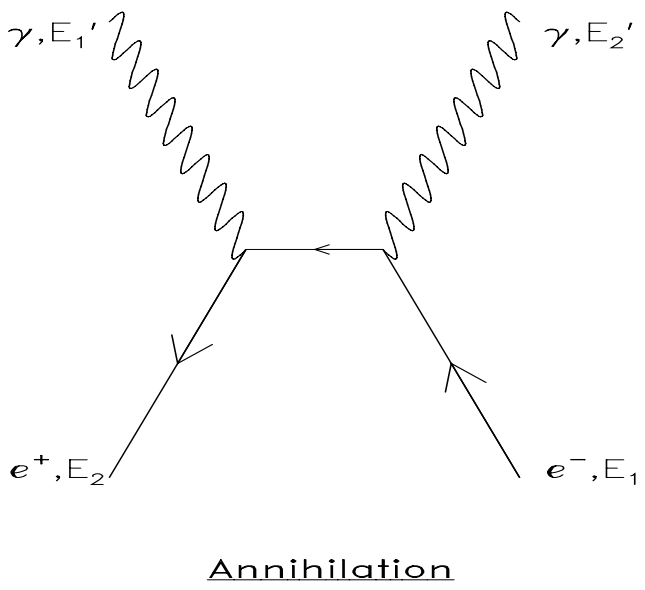

Figure 3: Two-photon positron annihilation.

EGS4 models two-photon "in-flight" annihilation employing the cross section formulae of Heitler [8]. Again, EGS4 considers the atomic electrons to be free, ignoring binding effects. EGS4 also ignores three and higher-photon annihilations ($e^+e^- \longrightarrow n\gamma[n > 2]$) as well as one-photon annihilation which is possible in the coulomb field of a nucleus ($e^+e^-\mathrm{N} \longrightarrow \gamma\mathrm{N}^*$). The higher-order processes are very much suppressed relative to the two-body process (by at least a factor of 1/137) while the one-body process competes with the two-photon process only at very high energies where the cross section becomes very small. If a positron survives until it reaches the transport cut-off energy `ECUT`, the EGS4 code then immediately converts it into two photons (annihilation at rest). No attempt is made to model the residual drift before annihilation.

3 Statistically grouped interactions

3.1 "Continuous" energy loss

EGS4 accounts for the energy loss to sub-threshold (soft bremsstrahlung below `AP`, collisions below `AE`) by assuming that this energy is lost continuously along its path. The formalism used by EGS4 is the Bethe-Bloch theory of charged particle energy loss [9, 10, 11] as expressed by Berger and Seltzer [12] and in ICRU 37 [5]. This continuous energy loss scales with the Z of the medium for the collision contribution and Z^2 for the radiative part. Charged particles can also polarise the media in which they travel. This "density effect" is important at high energies and for dense media. The default density effect parameters used by EGS4 came from a 1982 compilation by Sternheimer, Seltzer and Berger [13]. However, the user is at liberty to include other parameters if he chooses to. Recently, Duane *et al.* [14] have extended PEGS4 to input density effect tables in directly from the latest state-of-the-art compilations (as defined by the stopping-power guru Berger who distributes a PC-based stopping power program [15]).

Again, atomic binding effects are treated rather crudely by the Bethe-Bloch formalism. It assumes that each electron can be treated as if it were bound by an average binding potential. The use of more refined theories does not seem advantageous unless one wants to study electron transport below the K-shell binding energy of the highest atomic number element in the problem.

The stopping power versus energy for different materials is shown in fig. 4. The difference in the collision part is due mostly to the difference in ionisation potentials of the various atoms and partly to a $\overline{Z}/\overline{A}$ difference, because the vertical scale is plotted in MeV/(g/cm^2), a normalisation by atomic weight rather than electron density. Note that at high energy the argon line rises above the carbon line. Argon, being a gas, is reduced less by the density effect at this energy. The radiative contribution reflects mostly the relative Z^2 dependence of bremsstrahlung production.

The collisional energy loss by electrons and positrons is different for the same reasons described in the "catastrophic" interaction section. Annihilation is not treated as part of the positron slowing down process and is treated discretely as a "catastrophic" event. The differences are reflected in fig. 5, the positron/electron collision stopping power. EGS4 also ignores the reduction in the positron radiative stopping power. At 1 MeV this difference is a few percent in carbon and 60% in lead. This relative difference is depicted in fig. 6. A user must determine if his application will suffer from this shortcoming and interpret his results accordingly.

3.2 Multiple scattering

Elastic scattering of electrons and positrons from nuclei is predominantly small angle. If it were not for screening by the atomic electrons, the cross section would be infinite. The cross sections are, nonetheless, very large. There are several statistical theories that deal with multiple scattering. Some of these theories assume that the charged particle has interacted enough times so that they may be grouped together. The most popular such theory is the Fermi-Eyges theory [16], a small angle theory. This theory neglects large angle scattering and is unsuitable for accurate electron transport unless large angle scattering is somehow included (perhaps as a catastrophic interaction). The most accurate theory is that of Goudsmit and Saunderson [17, 18]. This theory does not require that many atoms participate in the production of a multiple scattering angle. However, calculation times required to produce few-atom distributions can

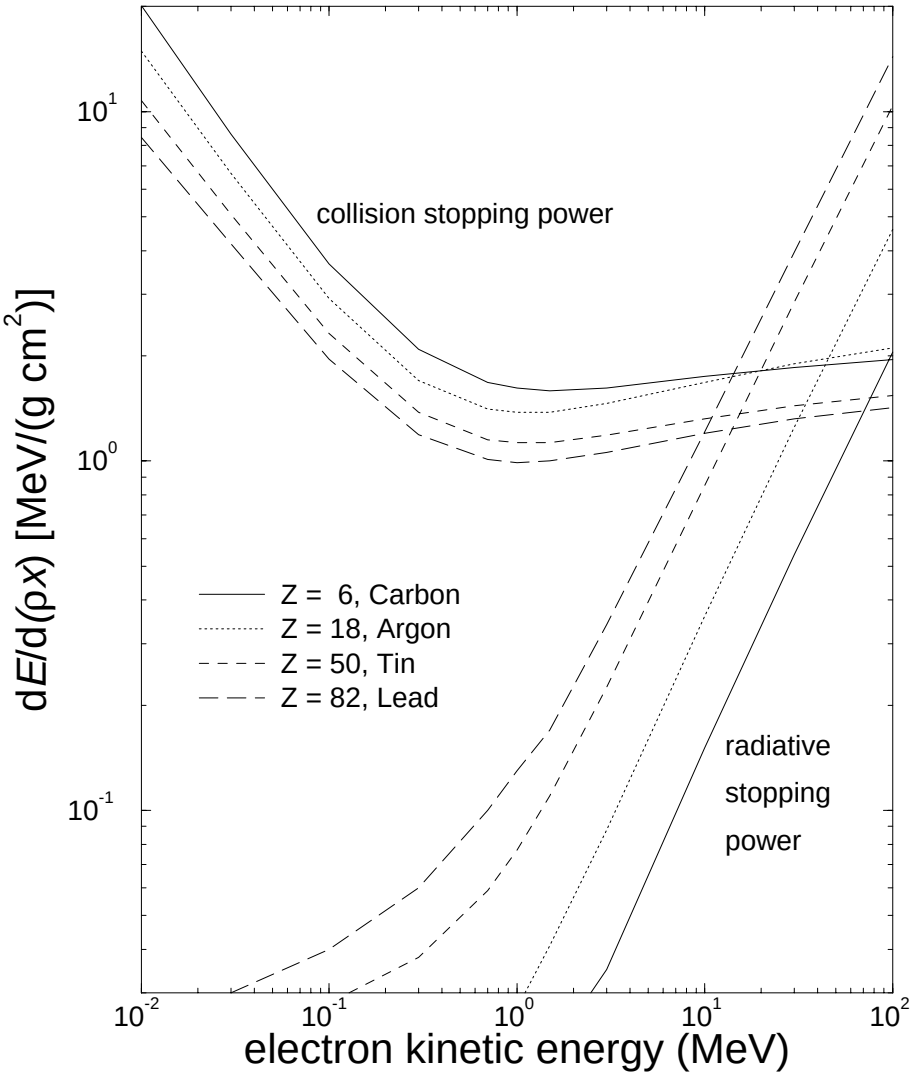

Figure 4: Stopping power *versus* energy.

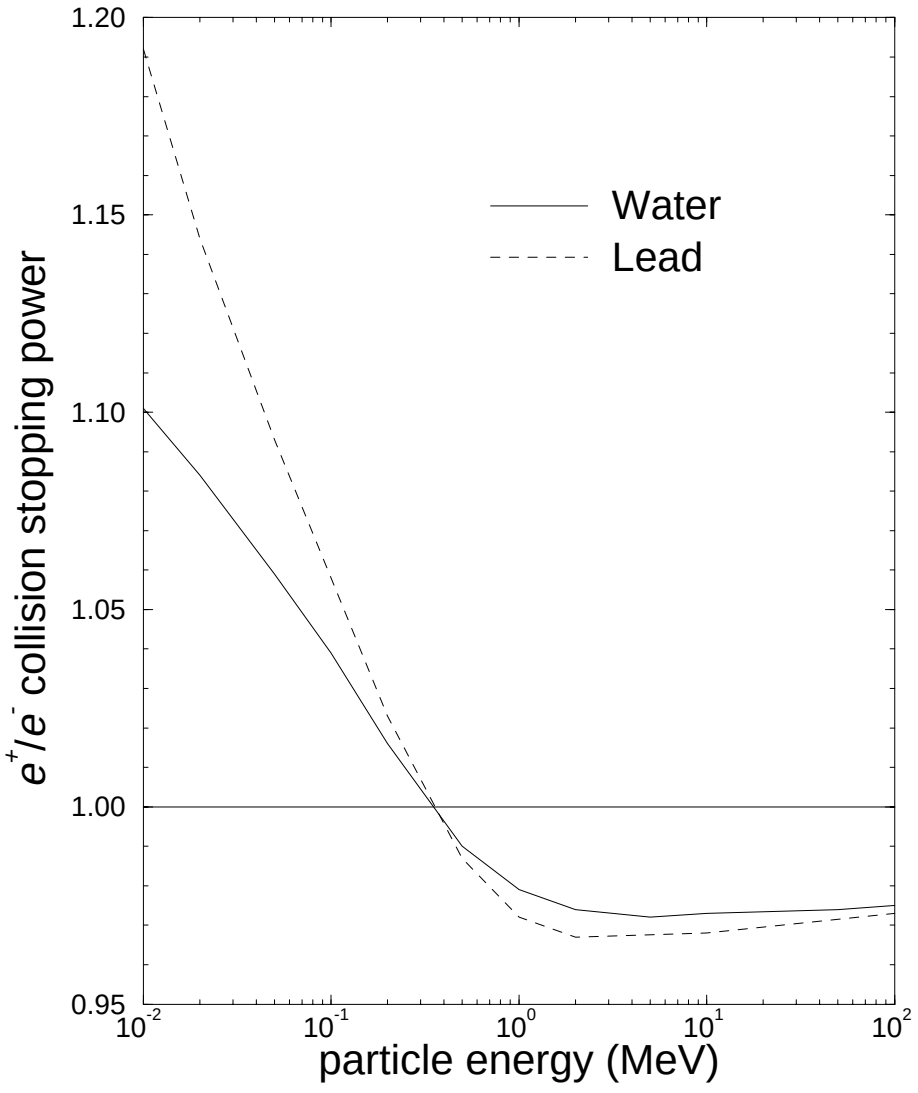

Figure 5: Positron/electron collision stopping power

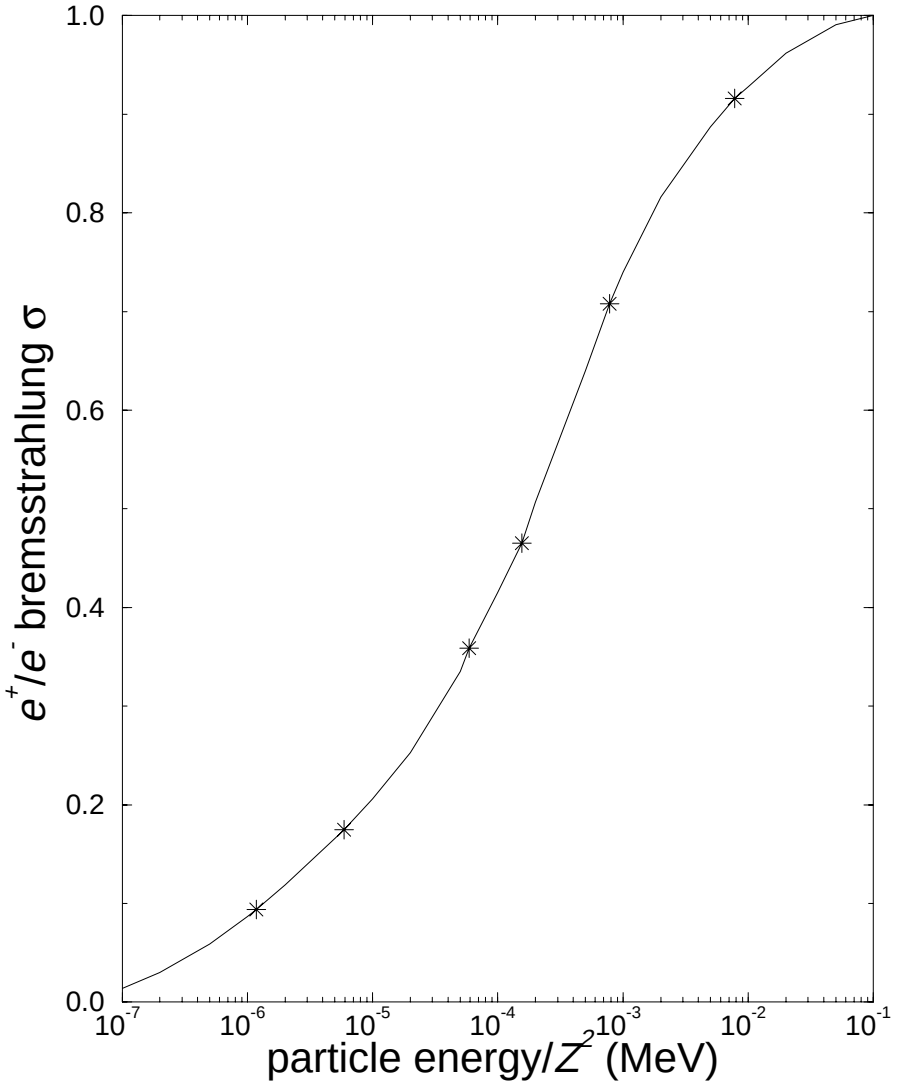

Figure 6: Positron/electron bremsstrahlung cross section.

get very long and have intrinsic numerical difficulties. Apart from accounting for energy-loss during the course of a step, there is no intrinsic difficulty with large steps either. The Goudsmit-Saunderson method is difficult to implement although it is the method of choice for the ETRAN based codes. EGS4 uses the Molière theory [19, 20] which is almost as good as Goudsmit-Saunderson and is easier to implement.

The Molière theory, although originally designed as a small angle theory has been modified to predict large angle scattering quite successfully [21]. The Molière theory includes the contribution of single event large angle scattering, for example, an electron backscatter from a single atom. The Molière theory ignores differences in the scattering of electrons and positrons, and uses the screened Rutherford cross sections instead of the more accurate Mott cross sections. However, the differences are known to be small. The Molière theory requires a minimum step-size as it is truly a "multiple" scattering theory, breaking down numerically if less than 25 atoms or so participate in the development of the angular distribution. Apart from accounting for energy loss, there is also a large step-size restriction because the Molière theory is couched in a small-angle formalism. Beyond this there are other corrections that can be applied [21, 22] but these have not been included in the EGS4 code. There is a much more complete discussion of Molière theory as applied in the EGS4 code in the Lecture "Step-size dependencies and PRESTA".

4 Electron transport

4.1 Typical electron tracks

A typical electron track as simulated by the EGS4 code is shown in fig. 7. An electron is

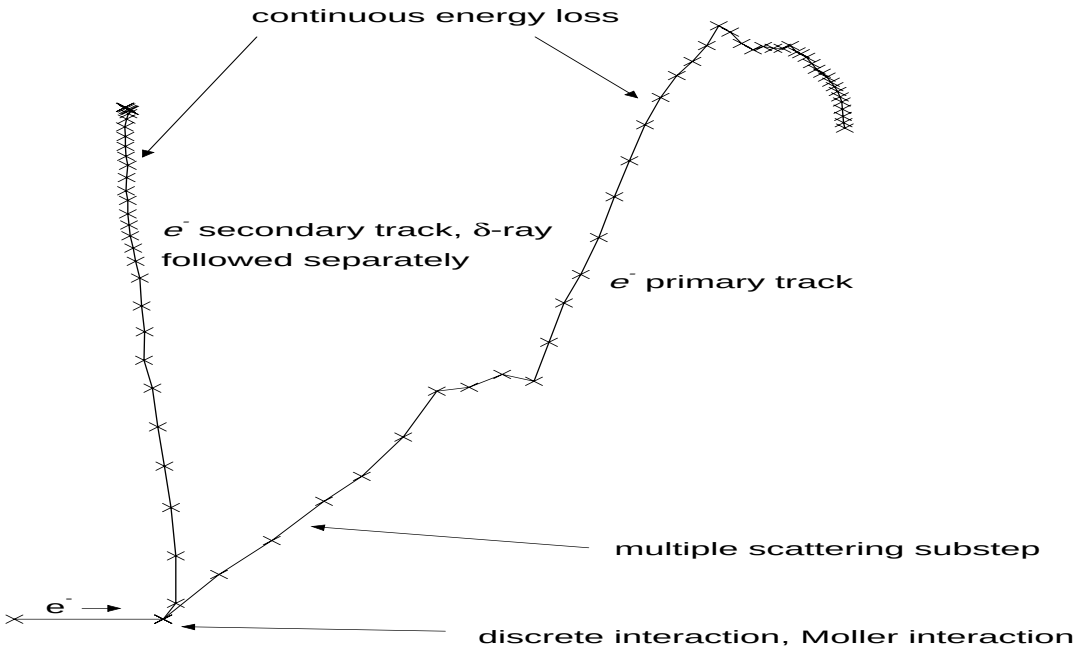

Figure 7: Typical electron track simulated by EGS4.

being transported through a medium. Along the way energy is being lost "continuously" to sub-threshold knock-on electrons and bremsstrahlung. The track is broken up into small "multiple

scattering" steps. In this case the length of these steps was chosen so that the electron lost 4% of its energy during each step. At the end of each of these steps the multiple scattering angle is selected according to the Molière distributions. Super-threshold events, here a single knock-on electron, sets other particles in motion. These particles are followed separately in the same fashion. The original particle, if it is does not fall below `ECUT`, is also transported. In general terms, this is exactly what the EGS4 electron transport logic simulates.

4.2 Typical multiple scattering steps

Now we demonstrate in fig. 8 what a multiple scattering step *should* look like.

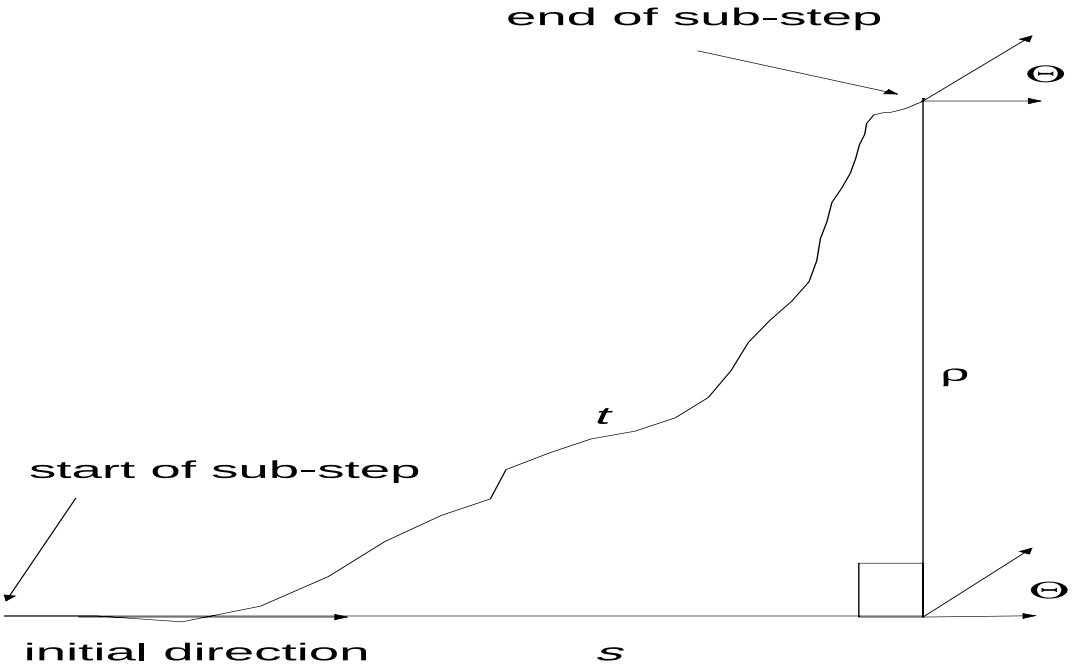

Figure 8: Typical multiple scattering step. Default EGS4 only simulates the straight-ahead portion and applies a crude approximation for the total curvature. EGS4 also ignores the lateral portion of the step.

In EGS4, a single electron step is characterised by the length of total curved path-length to the end point of the step, t. (This is a reasonable parameter to use because the number of atoms encountered along the way should be proportional to t.) At the end of the step the deflection from the initial direction, Θ, is sampled. Associated with the step is the average projected distance along the original direction of motion, s. In EGS4, s is related to t using the Fermi-Eyges [16] multiple scattering theory applied to the pathlength formalism of Yang [23]. (Details are given in the EGS4 manual.) The lateral deflection, ρ, the distance transported perpendicular to the original direction of motion, is ignored by the default version of EGS4. This is *not* to say that lateral transport is ignored by EGS4! Recalling fig. 7, we see that such lateral deflections do occur as a result of multiple scattering. It is only the lateral deflection during the course of a sub-step which is ignored. One can guess that if the multiple scattering steps are small enough, the electron track may be simulated more exactly. We shall see in a later lecture to what degree this is true and how careful choice of electron step-size is needed for accurate electron transport.

The Yang-Fermi-Eyges relation is also inaccurate, particularly at smaller energies and for large multiple scattering step-sizes. Additionally, s is a distributed quantity for a given t. These points are discussed in more detail in a further lecture.

EGS4 also ignores energy loss fluctuations for the sub-threshold continuous energy loss mechanisms. We shall see in the next section how calculated results are affected by this.

5 Examples of parameter selection

5.1 Thin water slab

As an example of the effect of secondary particle creation thresholds, consider an energy distribution of primary electrons, having started at 20 MeV and having passed through a 0.25 cm slab of water, and determined used different values of secondary particle creation thresholds. The spectra are given in fig. 9. In the CSDA calculation (circle), total stopping powers are employed, no secondaries were created and all electrons lose 618 keV. Setting `AE=1.511` (*i.e.* 1.0 MeV kinetic energy plus rest mass) allows secondary electrons to be set in motion with at least 1.0 MeV kinetic energy. This shifts the main peak upward (since restricted-collision total-radiative stopping powers are being used), and causes a 1 MeV gap below which there is a continuous distribution. If one disallows secondary electron creation but allows bremsstrahlung photon creation above 100 keV, (`AP=0.1`), one sees a different shift of the main peak (since total-collision restricted-radiative stopping powers are being used), and a 100 keV void between the main peak and the continuous distribution. Finally, with both secondary electron and photon creation (`AE=1.511, AP=0.001`), one still sees both thresholds in the primary energy spectrum.

If one wished to model the energy spectrum carefully one would have to set one's cutoffs to very low values. For this example, one reduces the thresholds to 1 keV, then no spurious thresholds are exhibited as seen in fig. 10. The distribution is exactly what one would calculate if one had used a proper implementation of the Landau [24] energy-straggling distribution.

5.2 Thick water slab

Low-threshold calculations are costly and not always needed. If one were interested in energy deposition in thick slabs, then one would be able to use relatively high values of secondary particle creation thresholds (up to a point!). For example, as seen in fig. 11 for the fall-off portion of a 20 MeV e^- depth-dose curve in water, there is not much sensitivity to the value of `AE`. Energy-deposition scoring integrates the differential energy spectra effectively obliterating details of the spectra.

Finally, consider the effect of the electron transport cutoff `ECUT`. In the example shown in fig. 12, 100 keV e^- were incident on a thick slab of water. In this case, `AE=0.521` and `ESTEPE=0.04` (discussed later in the step-size dependencies lecture). When an electron reaches the transport cutoff threshold, the history is terminated with all the residual kinetic energy deposited on the spot. This artificially compresses the depth dose curve. A good rule of thumb is to set `ECUT` so that the range of a discarded particle is a fraction of the resolution desired (*e.g.* $1/3^{\text{rd}}$ the depth-bin size in the problem).

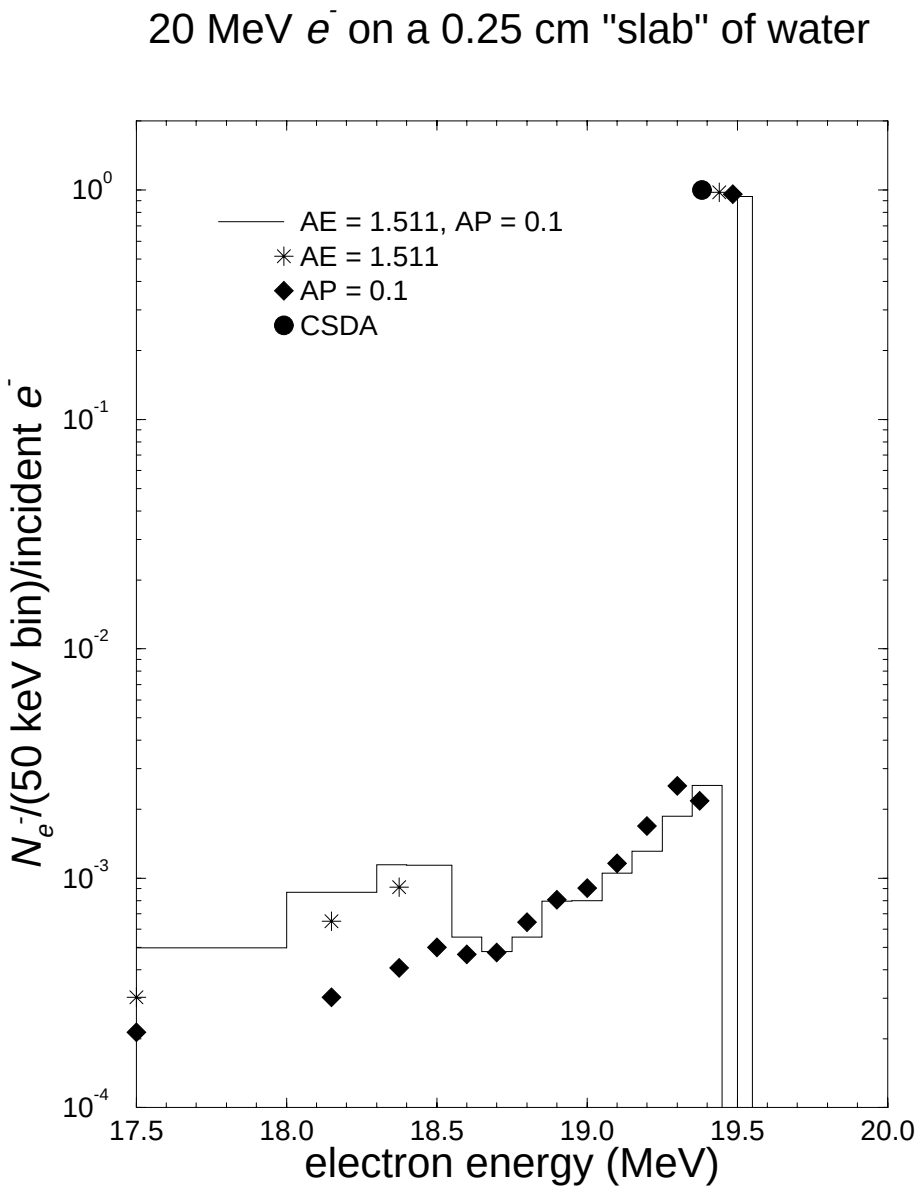

Figure 9: Energy distribution of primary electrons, starting at 20 MeV after passing through a 0.25 cm slab of water, calculated using different values of secondary particle creation thresholds. CSDA calculation (circle), `AE=1.511` (stars), `AP=0.1` (diamonds), `AE=1.511, AP=0.1` (histogram).

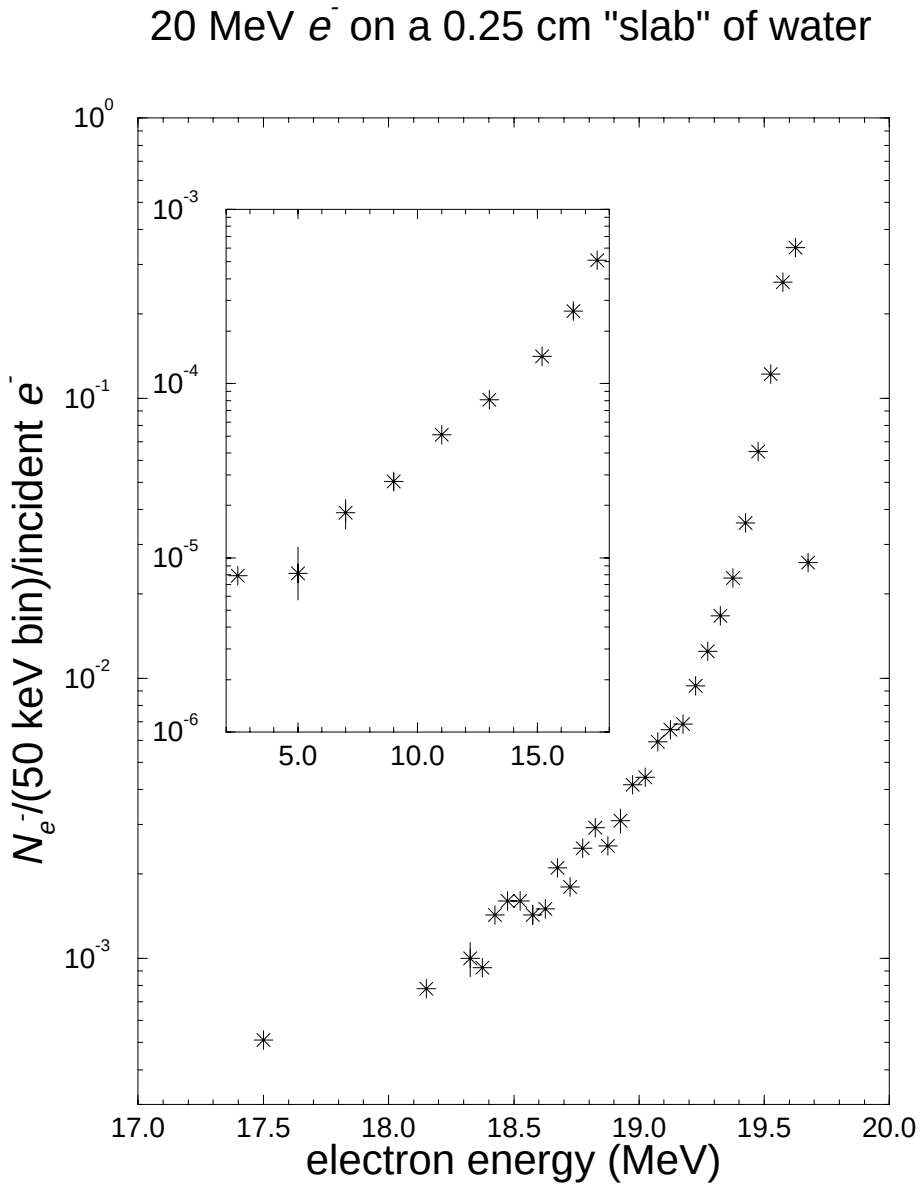

Figure 10: Energy distribution of primary electrons, starting at 20 MeV after passing through a 0.25 cm slab of water, calculated using low thresholds `AE=0.512, AP=0.001`. The distribution is exactly what one would calculate if one had used a proper implementation of the Landau [24] energy-straggling distribution.

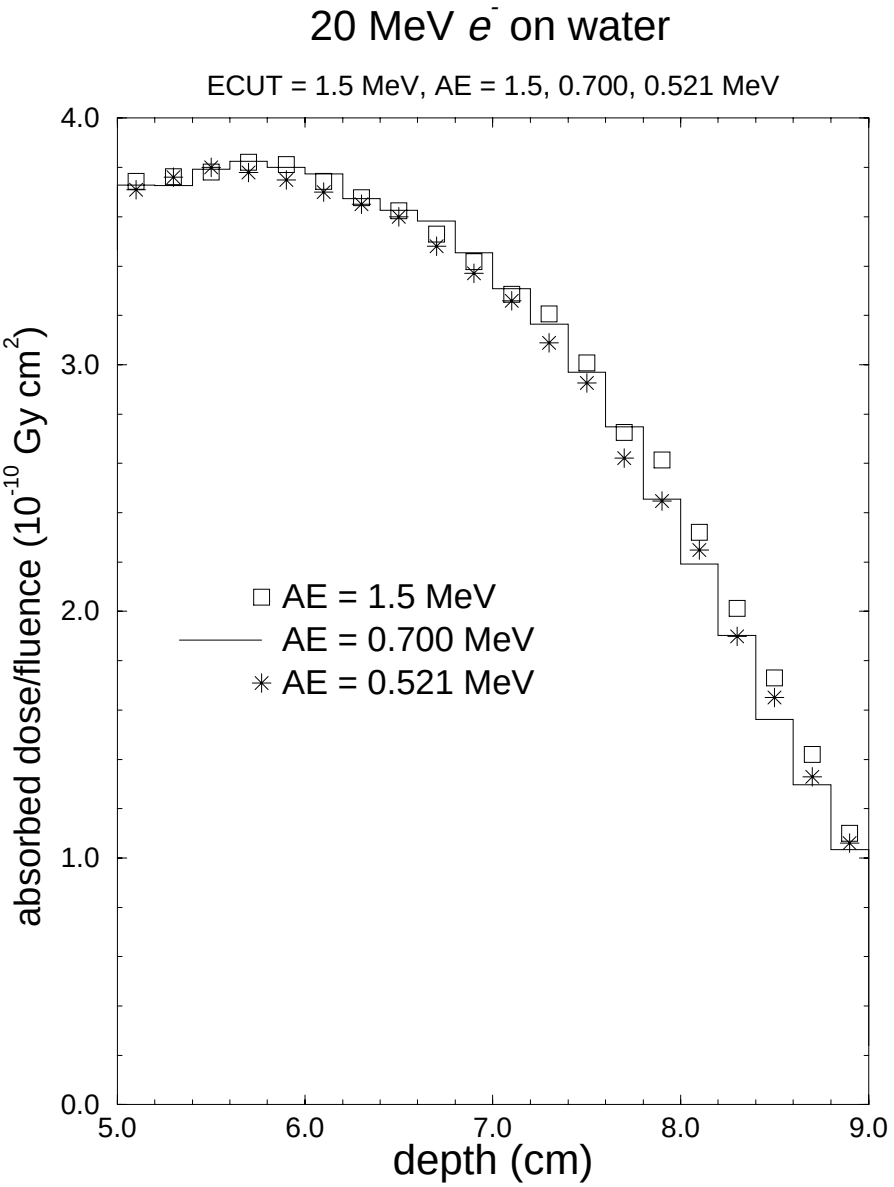

Figure 11: Fall-off portion of a 20 MeV e^- depth-dose in water for various values of the secondary electron threshold `AE`.

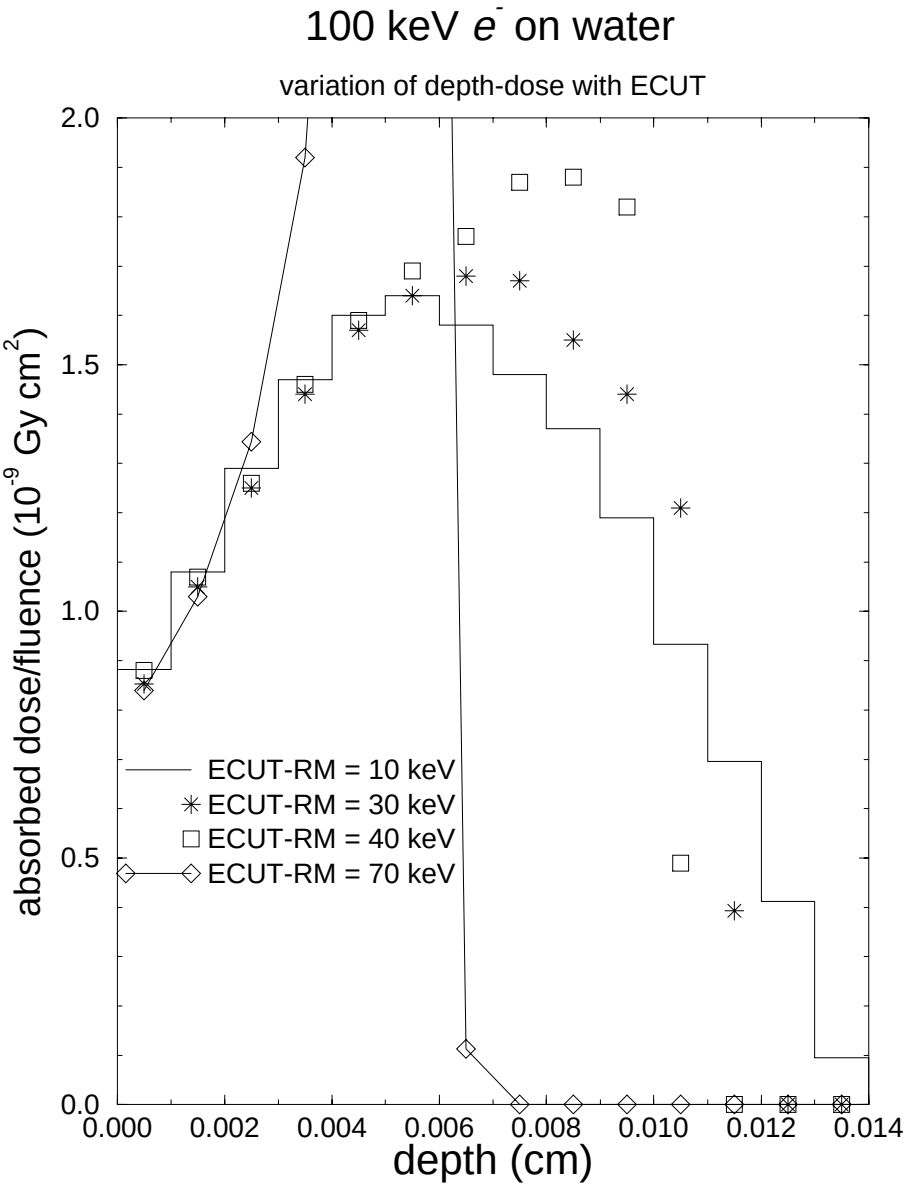

Figure 12: 100 keV e^- depth-dose in water for various values of the electron transport threshold `ECUT`.

6 Effect of physical modeling on a 20 MeV e^- depth-dose curve

In this section we will study the effects on the depth-dose curve of turning on and off various physical processes. Figure 13 presents two CSDA calculations (*i.e.* no secondaries are created and energy-loss straggling is not taken into account). For the histogram, no multiple scattering is modeled and hence there is a large peak at the end of the range of the particles because they all reach the same depth before being terminating and depositing their residual kinetic energy (189 keV in this case). Note that the size of this peak is very much a calculational artefact which depends on how thick the layer is in which the histories terminate. The curve with the stars includes the effect of multiple scattering. This leads to a lateral spreading of the electrons which shortens the depth of penetration of most electrons and increases the dose at shallower depths because the fluence has increased. In this case, the depth-straggling is entirely caused by the lateral scattering since every electron has travelled the same distance.

Figure 14 presents three depth-dose curves calculated with all multiple scattering turned off - *i.e.* the electrons travel in straight lines (except for some minor deflections when secondary electrons are created). In the cases including energy-loss straggling, a depth straggling is introduced because the actual distance travelled by the electrons varies, depending on how much energy they give up to secondaries. Two features are worth noting. Firstly, the energy-loss straggling induced by the creation of bremsstrahlung photons plays a significant role despite the fact that far fewer secondary photons are produced than electrons. They do, however, have a larger mean energy. Secondly, the inclusion of secondary electron transport in the calculation leads to a dose buildup region near the surface. Figure 15 presents a combination of the effects in the previous two figures. The extremes of no energy-loss straggling and the full simulation are shown to bracket the results in which energy-loss straggling from either the creation of bremsstrahlung or knock-on electrons is included. The bremsstrahlung straggling has more of an effect, especially near the peak of the depth-dose curve.

7 Electron transport logic

Figure 16 is a schematic flow chart showing the essential differences between different kinds of electron transport algorithms. EGS4 is a class II algorithm which samples interactions discretely and correlates the energy loss to secondary particles with an equal loss in the energy of the primary electron (positron).

There is a close similarity between this flow chart and EGS4's photon transport flow chart. The essential differences are the nature of the particle interactions as well as the additional continuous energy-loss mechanism and multiple scattering. Positrons are treated by the same subroutine in EGS4 although it is not shown in fig. 16.

Imagine that an electron's parameters (energy, direction, etc.) are on top of the particle stack. (`STACK` is an EGS4 array containing the phase-space parameters of particles awaiting transport.) The electron transport routine, `ELECTR`, picks up these parameters and first asks if the energy of this particle is greater than the transport cutoff energy, `ECUT`. If it is not, the electron is discarded. (This is not to that the particle is simply thrown away! "Discard" means that the scoring routines are informed that an electron is about to be taken off the transport stack.) If there is no electron on the top of the stack, control is given to the photon transport routine. Otherwise, the next electron in the stack is picked up and transported. If the original electron's energy was great enough to be transported, the distance to the next catastrophic interaction point is determined, exactly as in the photon case. The multiple scattering step-

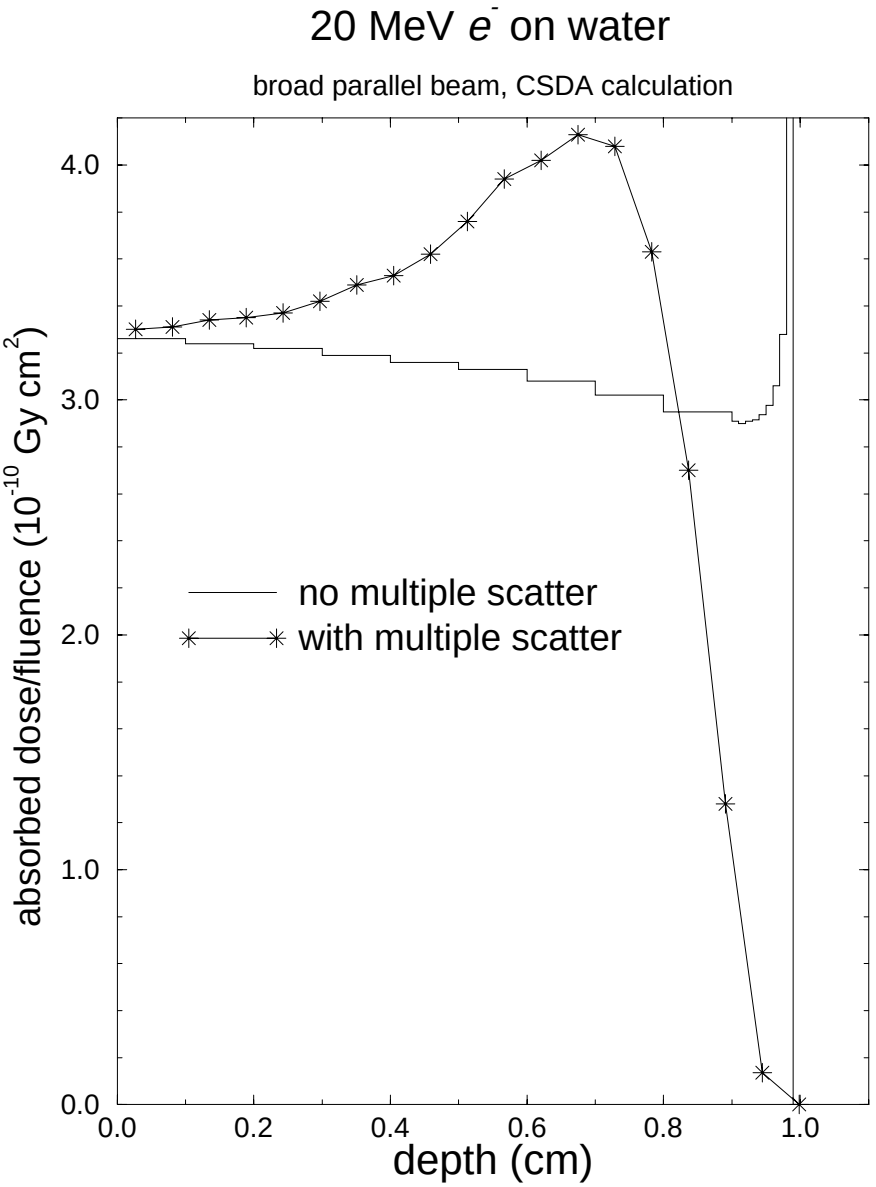

Figure 13: Depth-dose curve for a broad parallel beam (BPB) of 20 MeV electrons incident on a water slab. The histogram represents a CSDA calculation in which multiple scattering has been turned off, and the stars show a CSDA calculation which includes multiple scattering.

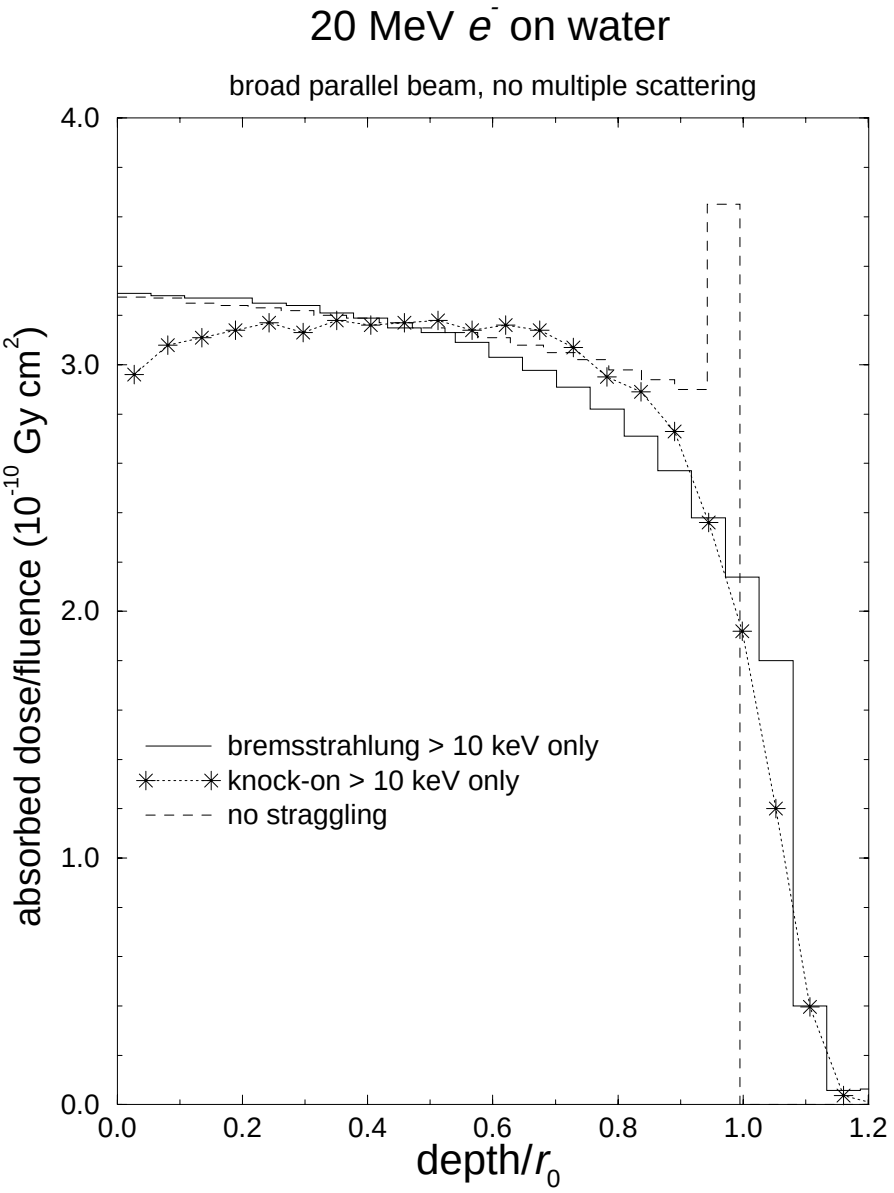

Figure 14: Depth-dose curves for a BPB of 20 MeV electrons incident on a water slab, but with multiple scattering turned off. The solid histogram calculation models no straggling and is the same simulation as given by the histogram in fig. 13. Note the difference caused by the different bin size. The dashed histogram includes energy-loss straggling due to the creation of bremsstrahlung photons with an energy above 10 keV. The curve denoted by the stars includes only that energy-loss straggling induced by the creation of knock-on electrons with an energy above 10 keV.

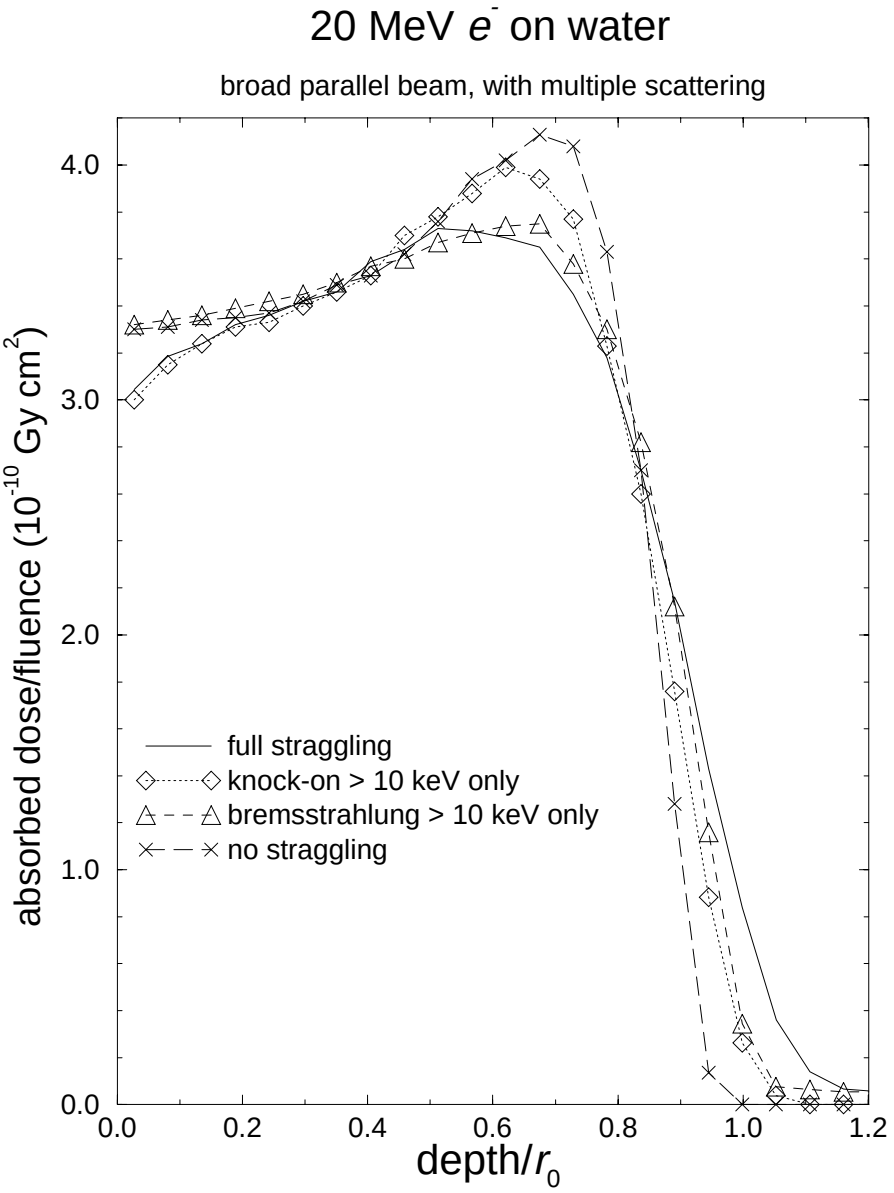

Figure 15: BPB of 20 MeV electrons on water with multiple scattering included in all cases and various amounts of energy-loss straggling included by turning on the creation of secondary photons and electrons above a 10 keV threshold.

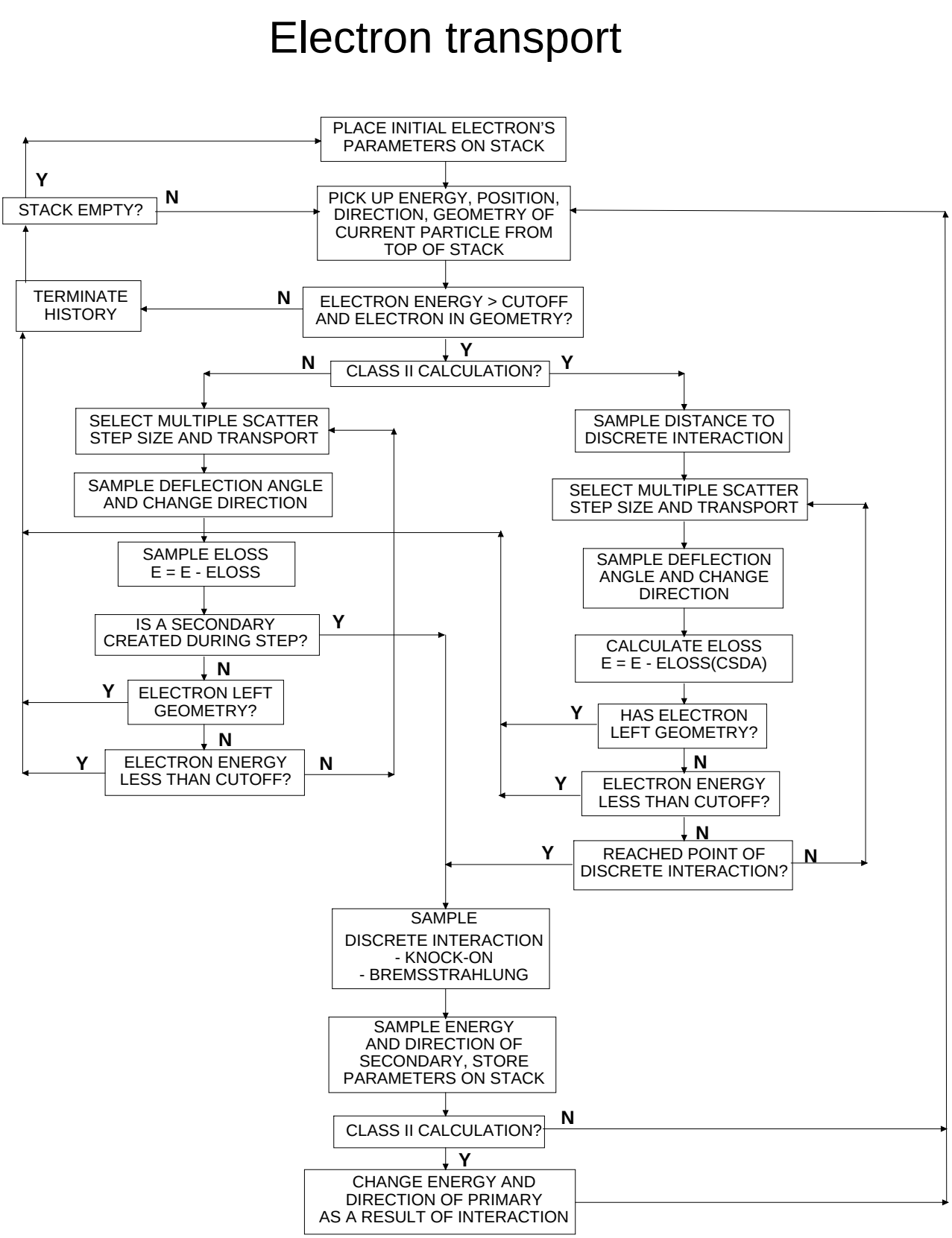

Figure 16: Flow chart for electron transport. Much detail is left out.

size t is then selected and the particle transported, taking into account the constraints of the geometry and the limits of the Molière theory. It is at this point that EGS4 calculates s, given t. After the transport, the multiple scattering angle is selected and the electron's direction adjusted. The continuous energy loss is then deducted. If the electron, as a result of its transport, has left the geometry defining the problem, it is discarded. Otherwise, its energy is tested to see if it has fallen below the cutoff as a result of its transport. If the electron has not yet reached the point of interaction a new multiple scattering step is effected. This innermost loop undergoes the heaviest use in most calculations because often many multiple scattering steps occur between points of interaction (see fig. 7). If the distance to a discrete interaction has been reached, then the type of interaction is chosen. Secondary particles resulting from the interaction are placed on the stack as dictated by the differential cross sections, lower energies on top to prevent stack overflows. The energy and direction of the original electron are adjusted and the process starts all over again.

This is merely a bare outline of the electron transport routine in EGS4. The interested student is urged to seek out more detail in the EGS4 manual, particularly the photon and electron flow charts in Appendix A.

References

[1] H.W. Koch and J.W. Motz, *Bremsstrahlung cross-section formulas and related data*, Rev. Mod. Phys. **31** 920 – 955 (1959).

[2] H. Davies, H.A. Bethe and L.C. Maximon, *Theory of Bremsstrahlung and Pair Production. II. Integral Cross Sections for Pair Production*, Phys. Rev. **93** 788 (1954).

[3] Y.S. Tsai, *Pair Production and Bremsstrahlung of Charged Leptons*, Rev. Mod. Phys. **46** 815 (1974).

[4] D.W.O. Rogers, S. Duane, A.F. Bielajew, W.R. Nelson, *Use of ICRU-37/NBS radiative stopping powers in the EGS4 system*, National Research Council of Canada report PIRS-0177 (1989).

[5] ICRU, *Stopping Powers for Electrons and Positrons*, Report 37, Bethesda MD (1984).

[6] S.M. Seltzer and M.J. Berger, *Bremsstrahlung spectra from electron interactions with screened atomic nuclei and orbital electrons*, Nucl. Inst. Meth. Phys. Res. B**12** 95 – 134 (1985).

[7] A.F. Bielajew, R. Mohan and C.S. Chui, *Improved bremsstrahlung photon angular sampling in the EGS4 code system*, National Research Council of Canada Report PIRS-0203 (1989).

[8] W. Heitler, *The Quantum Theory of Radiation*, (Clarendon Press, Oxford) (1954).

[9] H.A. Bethe, *Theory of passage of swift corpuscular rays through matter*, Ann. Physik **5** 325 (1930).

[10] H.A. Bethe, *Scattering of electrons*, Z. für Physik **76** 293 (1932).

[11] F. Bloch, *Stopping power of atoms with several electrons*, Z. für Physik **81** 363 (1933).

[12] M.J. Berger and S.M. Seltzer, *Tables of energy losses and ranges of electrons and positrons*, NASA Report SP-3012 (Washington DC) (1964).

[13] R.M. Sternheimer, S.M. Seltzer and M.J. Berger, *Density effect for the ionization loss of charged particles in various substances*, Phys Rev B**26** 6067 (1982).

[14] S. Duane, A.F. Bielajew and D.W.O. Rogers, *Use of ICRU-37/NBS Collision Stopping Powers in the EGS4 System*, NRCC Report PIRS-0177, Ottawa, March (1989).

[15] M.J. Berger, *ESTAR, PSTAR and ASTAR: Computer Programs for Calculating Stopping-Power and Ranges for Electrons, Protons, and Helium Ions*, NIST Report NISTIR-4999 (Washington DC) (1992).

[16] L. Eyges, *Multiple scattering with energy loss*, Phys. Rev. **74** 1534 (1948).

[17] S.A. Goudsmit and J.L. Saunderson, *Multiple Scattering of Electrons*, Phys. Rev. **57** 24 – 29 (1940).

[18] S.A. Goudsmit and J.L. Saunderson, *Multiple Scattering of Electrons. II*, Phys. Rev. **58** 36 – 42 (1940).

[19] G.Z. Molière, *Theorie der Streuung schneller geladener Teilchen. I. Einzelstreuung am abgeschirmten Coulomb-Field*, Z. Naturforsch **2a** 133 – 145 (1947).

[20] G.Z. Molière, *Theorie der Streuung schneller geladener Teilchen. II. Mehrfach- und Vielfachstreuung*, Z. Naturforsch **3a** 78 – 97 (1948).

[21] H.A. Bethe, *Molière's theory of multiple scattering*, Phys. Rev. **89** 1256 – 1266 (1953).

[22] K.B. Winterbon, *Finite-angle multiple scattering*, Nuclear Instruments and Methods **B21** 1 – 7 (1987).

[23] C.N. Yang, *Actual path length of electrons in foils*, Phys. Rev **84** 599 – 600 (1951).

[24] L. Landau, *On the energy loss of fast particles by ionization*, J. Phys. USSR, **8** 201 (1944).